JOURNAL OF GEOPHYSICAL RESEARCH, VOL. 93, NO. C8, PAGES 9261–9269, AUGUST 15, 1988

Eulerian Measurements of Horizontal Accelerations in Shoaling Gravity Waves

STEVE ELGAR

Electrical and Computer Engineering, Washington State University, Pullman

R. T. GUZA

Center for Coastal Studies, Scripps Institution of Oceanography, La Jolla, California

M. H. FREILICH

Jet Propulsion Laboratory, California Institute of Technology, Pasadena

Laboratory and field measurements of suspended sediment in the nearshore suggest that fluid accelerations are an important factor in sediment transport by oscillatory waves. Here, Eulerian accelerations of the cross-shore velocity are calculated from measurements of velocity obtained by an array of bottom-mounted electromagnetic flow meters spanning a natural surf zone. Large shoreward accelerations of brief duration are associated with the steep front faces of both near-breaking and breaking waves. Weaker offshore accelerations of longer duration occur during passage of the more gently sloped rear faces. The acceleration field is thus strongly skewed in the shoreward direction. Power spectra and bispectra indicate, as expected, that statistics of the acceleration field are significantly influenced by high-frequency motions but are rather insensitive to surf beat.

1. INTRODUCTION

On the basis of a comprehensive review of laboratory studies of sediment transport by oscillatory flow, *Hallermeier* [1982] concluded that "a direct role of fluid acceleration in sand transport by oscillatory flow seems unequivocally to have been established." The flows considered were primarily sinusoidal, and *Hallermeier* [1982, equation 5] developed an expression relating time-averaged gross sediment transport volume to peak acceleration. Since instantaneous transport was not measured, the temporal dependence of transport on instantaneous acceleration could not be specified. This was not particularly important for sinusoidal flows in the laboratory because the entire time history of accelerations was determined by the peak acceleration. However, it is unclear from Hallermeier's results how sediment transport depends on accelerations in an asymmetric, random wave field.

There are surprisingly few published field measurements of wave-induced horizontal fluid accelerations. *Ewing et al.* [1987] present field measurements of the vertical accelerations at the free surface of deep water wind waves. *Hanes and Huntley* [1986] deployed both an electromagnetic flow meter and an optical backscatter sensor which continuously measured suspended sediment concentration at a single location well seaward of the surf zone on a natural beach. They noted that increases in suspended sediment concentration occurred more often during onshore than offshore flows, even though these flows were of approximately equal speed. In their data the strongest accelerations (and decelerations) occurred during onshore flows, and *Hanes and Huntley* [1986] tentatively concluded that "suspension . . . may be determined by fluid acceleration more than velocity," as suggested by theoretical work. On the other hand, the field data presented below indicate that immediately seaward of the breaking region and in the surf zone, large accelerations do not necessarily coincide with onshore flows. The objective of this paper is to analyze a set of field observations of near-bottom fluid accelerations in the shoaling region and surf zone of a single beach. Hopefully, this description of the magnitudes, asymmetries, and cross-shore variations of acceleration statistics in a typical natural surf zone will be useful background information when acceleration-dependent models of sediment transport under random waves are formulated. In section 2 the field experiment and data reduction are briefly described. Acceleration variance and spectra are considered in section 3, and asymmetries in the acceleration field are described in section 4. A discussion and conclusions follow in section 5.

Paper number 8C0295.
0148-0227/88/008C-0295$05.00

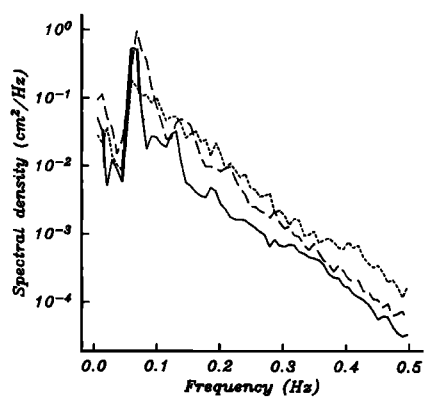

Fig. 1. Autospectra of bottom pressure in approximately 3.8-m depth: solid line, February 2 (256 dof); long dashes, February 3 (208 dof); short dashes, February 15 (80 dof).

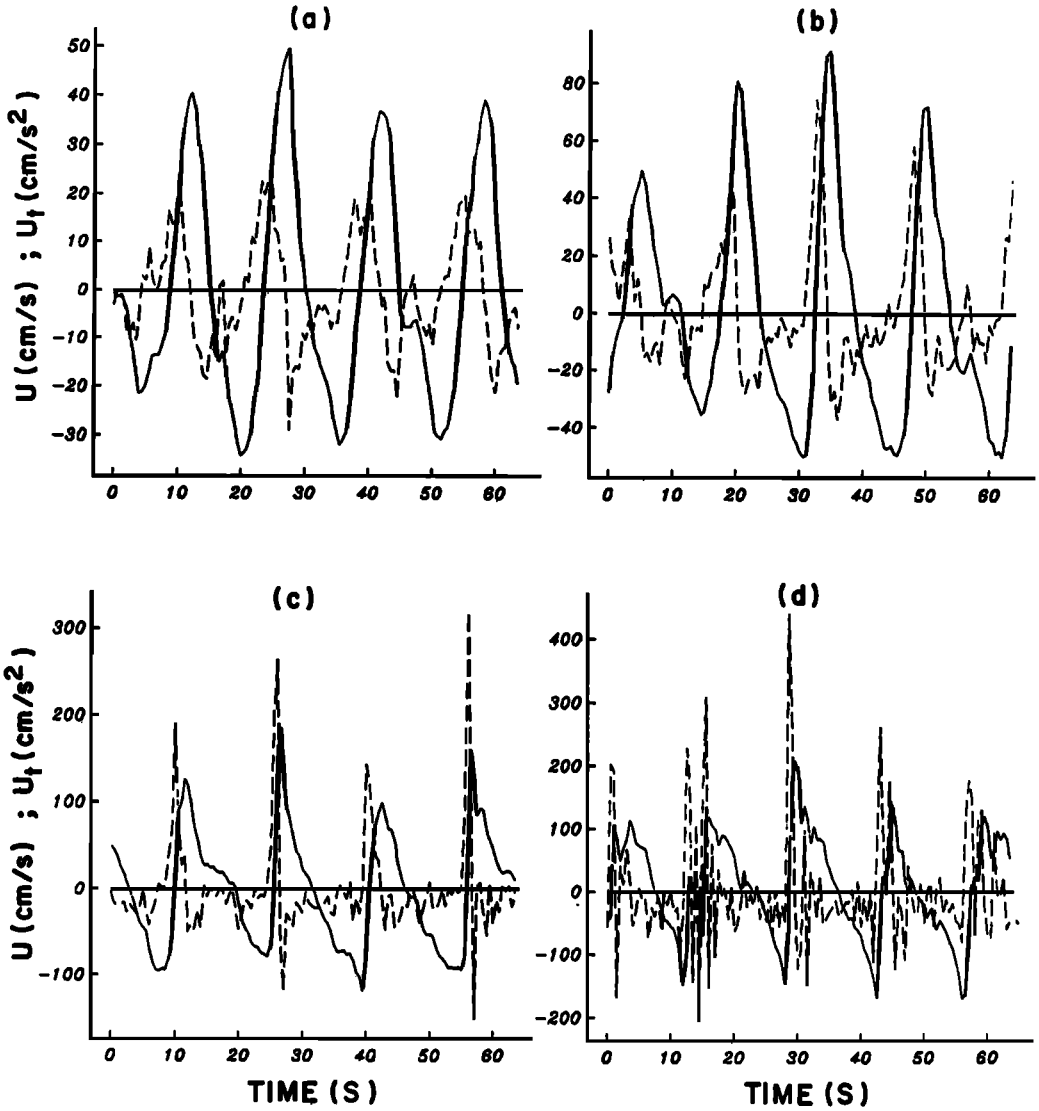

Fig. 2. Observed cross-shore velocity (solid line) and calculated acceleration (dashed line) versus time for a short section of the February 2 data. Depths are (*a*) 6.3 m, (*b*) 3.3 m, (*c*) 1.5 m, and (*d*) 0.9 m. Positive velocities are directed onshore.

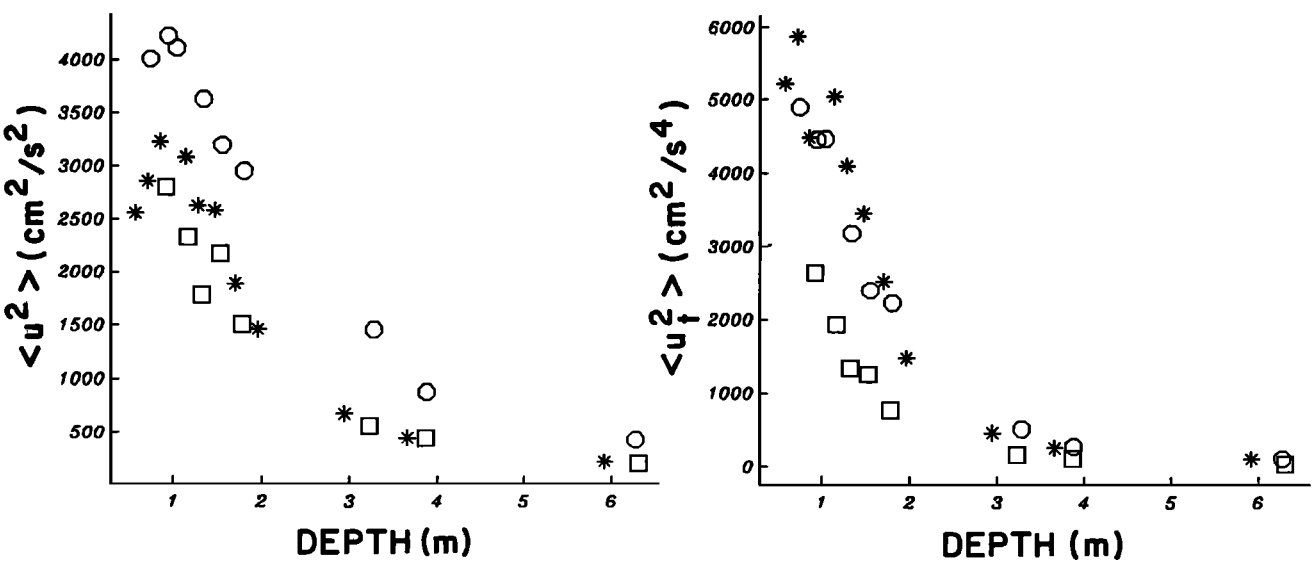

Fig. 3. (left) Cross-shore velocity and (right) acceleration variance versus depth. Symbols are as follows: Squares, February 2; circles, February 3; asterisks, February 15.

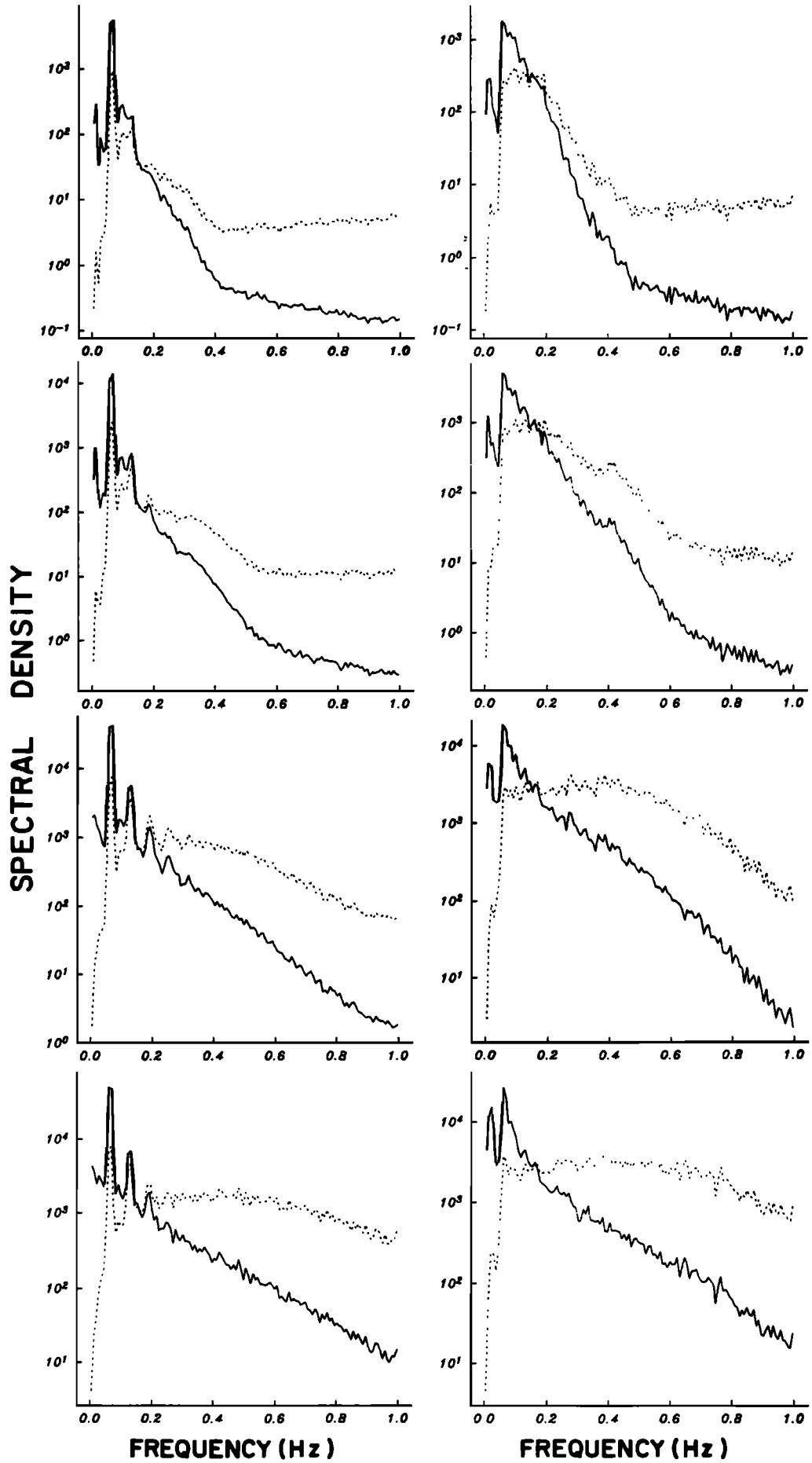

Fig. 4. Autospectra of cross-shore velocity (solid line, $(cm/s)^2/Hz$) and acceleration (dashed line, $(cm/s^2)^2/Hz$) for (left) February 2 (256 dof) and (right) February 15 (80 dof). Approximate depths are, from top to bottom, $h = 6.3$, 3.3, 1.5, and 0.9 m for February 2 and $h = 5.9$, 2.9, 1.5, and 0.9 m for February 15.

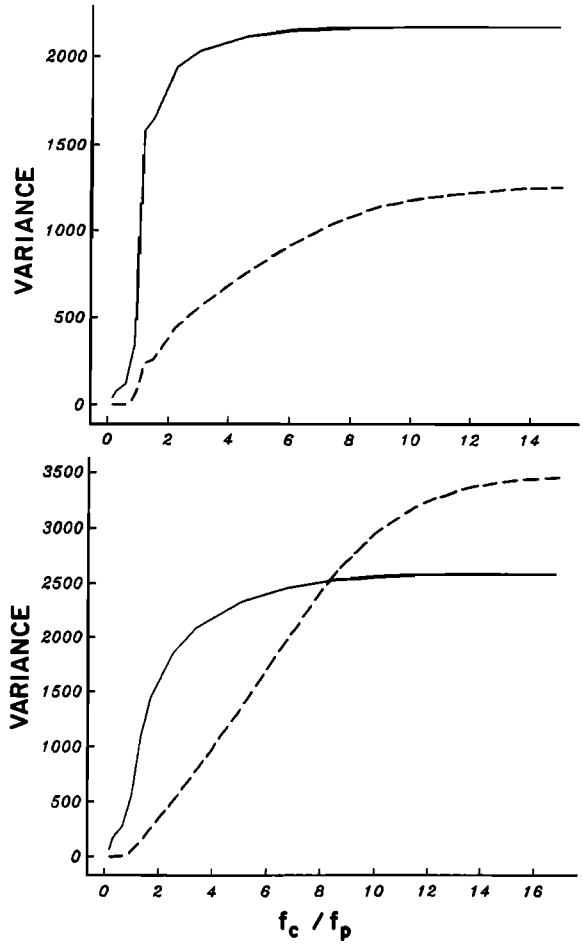

Fig. 5. Cross-shore velocity ((cm/s)^2, solid line) and acceleration ((cm/s^2)^2, dashed line) variance versus the ratio of high-frequency cutoff f_c to the power spectral peak frequency f_p for (top) February 2 (f_p = 0.067 Hz) and (bottom) February 15 (f_p = 0.059 Hz) in approximately 1.5-m depth. February 3 is similar to February 2.

2. Experiment and Data Reduction

The present study utilizes measurements from an array of 12 electromagnetic current meters deployed on a cross-shore transect at Leadbetter Beach, Santa Barbara, California, during February 1980. The meters were Marsh-McBirney model 512, with 4-cm-diameter spherical probes. The sensing elements were positioned about 50 cm above the seabed in mean depths ranging from about 1 to 6 m. The measurements presented here are from instruments that remained submerged throughout a data run. Thus data from the inner surf zone where current meters were alternately submerged and exposed are not considered.

The bottom contours in very shallow water were relatively straight and parallel, and the mean foreshore slope was roughly 0.05. Beach profiles, plan views of the nearshore bathymetry and sensor positions, and a general description of the directional properties of the wave field are given by *Thornton and Guza* [1986], *Guza et al.* [1986], and references therein.

Data were sampled at 2 Hz for between 0.7 and 2.4 hours spanning high tide, and subdivided into sections of 512-s duration. The filters in the flow meter electronics have a 4-Hz corner frequency and have only a small effect (6% reduction) on the power at the Nyquist frequency (1 Hz). Frequency smoothing was performed on spectra and bispectra, yielding a final frequency resolution of 0.0078 Hz. Statistics were calculated for each short section and then ensemble averaged over the collection of sections for each day, yielding between 80 and 256 degrees of freedom (dof), depending on the number of short sections ensembled. Various statistical tests [*Elgar and Guza*, 1985*a*] were used to verify stationarity.

Three days (February 2, 3, and 15, 1980) were selected for analysis. Significant wave heights in 4-m depth (outside the zone of wave breaking) were 60, 93, and 65 cm, respectively. Swell from a distant storm resulted in a relatively narrow sea surface elevation spectrum on February 2 and 3, while local wave generation contributed to a broader spectrum on February 15 (Figure 1). Various aspects of the nearshore waves and currents on these days have been previously discussed: the evolution of the spectra, cross spectra, and bispectra of sea surface elevation [*Elgar and Guza*, 1985*a*, *b*], the spatial variation of wave height and longshore currents [*Thornton and Guza*, 1986], and the wave number–frequency spectra of low-frequency surf beat [*Oltman-Shay and Guza*, 1987].

For the purposes of this study, the seaward edge of the breaking region was defined qualitatively as the most shoreward location where the wave field's linear energy flux was 85% of the flux in 4-m depth. The depths corresponding to this location were approximately 1.3, 1.6, and 1.4 m for February 2, 3, and 15, respectively.

Because of refraction, the oscillating currents of surface waves in shallow water are strongly polarized in the cross-shore direction. The principal wave direction in 4-m depth has been estimated as less than 20° [*Elgar and Guza*, 1985*a*, Figure 12; *Thornton and Guza*, 1986, Table 1] for each of these data sets. Time series of Eulerian accelerations were therefore obtained from cross-shore velocity measurements by numerical differentiation. The time series of cross-shore currents were Fourier transformed, the complex amplitudes were multiplied by $i\omega$ (where ω is the radian frequency of each Fourier component), and the resulting coefficients were inverse Fourier transformed. Essentially the same method was used by *Ewing et al.* [1987] to obtain Eulerian vertical accelerations of the free surface by twice differentiating time series of sea surface elevation. Windowing of the original time series is necessary to prevent spurious accelerations from being calculated near the end points, owing to mismatches in levels at the two ends of the time series. However, for the field measurements considered here, tests showed that the overall statistics were essentially unchanged even in the absence of windowing.

3. Acceleration Variance and Spectra

Example time series of velocity u and acceleration u_t are shown in Figure 2. Large accelerations are associated with the passage of both unbroken and broken waves with steep faces. Near-bottom velocity and acceleration variances increase with decreasing depth (Figure 3). These increases are associated with the reduced hydrodynamic attenuation of high-frequency components (i.e., filtering by the water column), linear shoaling effects (i.e., conservation of energy flux), and the resonant excitation of high frequency spectral components during shoaling [*Freilich and Guza*, 1984; *Elgar and Guza*, 1985*a*, *b*, 1986]. For the frequency band 0.04 to 0.3 Hz (where the waves are progressive and correction for depth attenuation does not artificially enhance high-frequency noise) linear finite depth theory accounts for about 90% of the increase in velocity

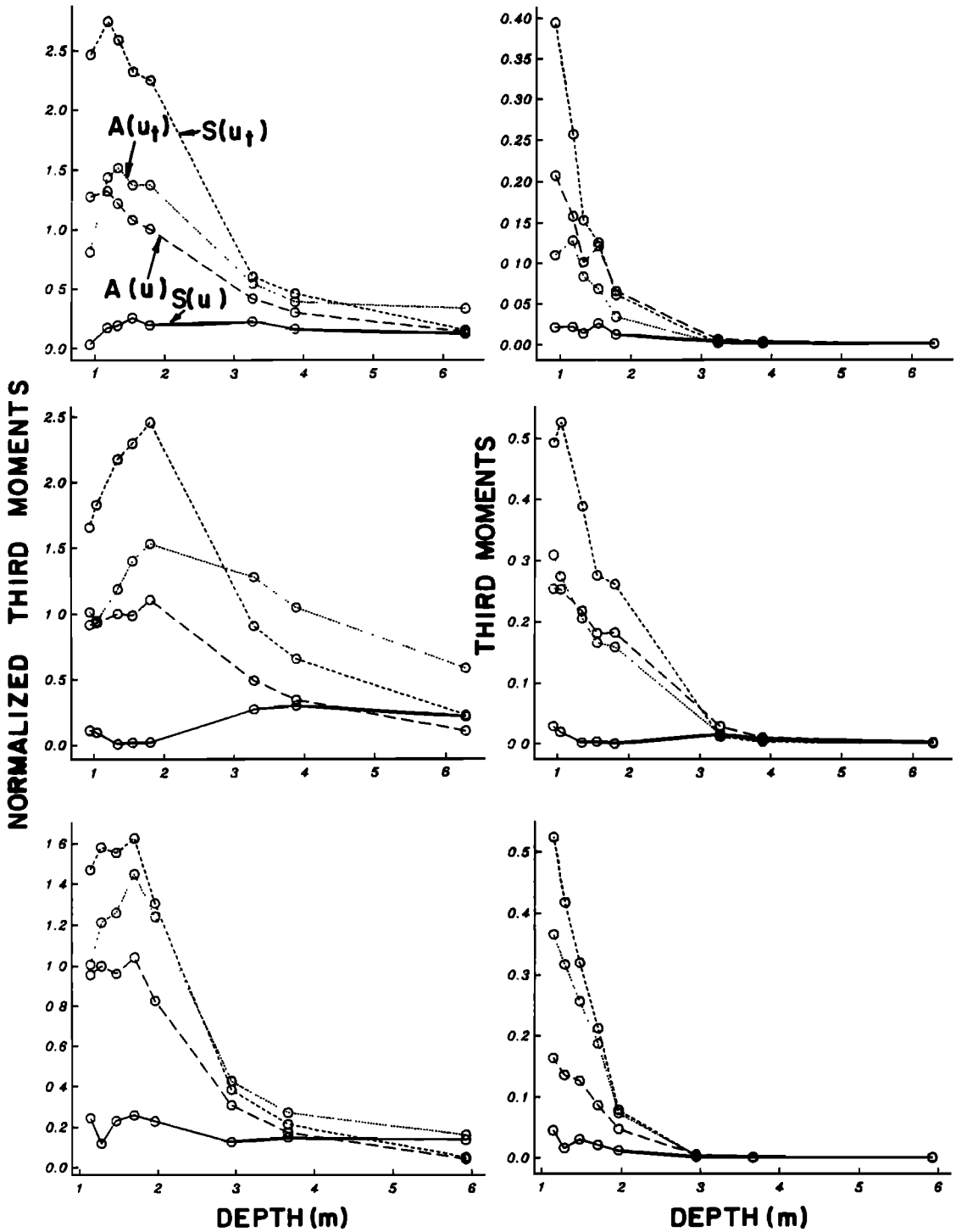

Fig. 6. (left) Normalized third moments (equation (1)) and (right) dimensional third moments (equation (1) without the denominator) versus depth for (top) February 2, (middle) February 3, and (bottom) February 15. The solid line shows $S(u)$; long dashes, $A(u)$; short dashes, $S(u_t)$; and dots, $A(u_t)$ (see top left). Units for dimensional moments are $(m/s)^3$ and $(m/s^2)^3$ for u and u_t, respectively. For the coordinate system used here, $A(u_t)$ is negative (except at the deepest sensors) and has been multiplied by -1 for convenience of figure display.

variance on all days and from about 60% (February 15) to 80% (February 2) of the increase in acceleration variance between the deepest sensor (approximately 6 m depth) and the seaward edge of the breaking region.

Representative u and u_t spectra for February 2 and 15 (Figure 4) show that high-frequency motions contribute moderately to velocity variance and significantly to acceleration variance, and the importance of motions at these frequencies increases as the waves shoal. *Ewing et al.* [1987] show that estimates of variances of both the Eulerian and Lagrangian surface vertical acceleration for deepwater waves depend on the high-frequency cutoff used in the calculations. For the data considered here, at the seaward edge of the surf zone the velocity and acceleration variances depend on frequencies up

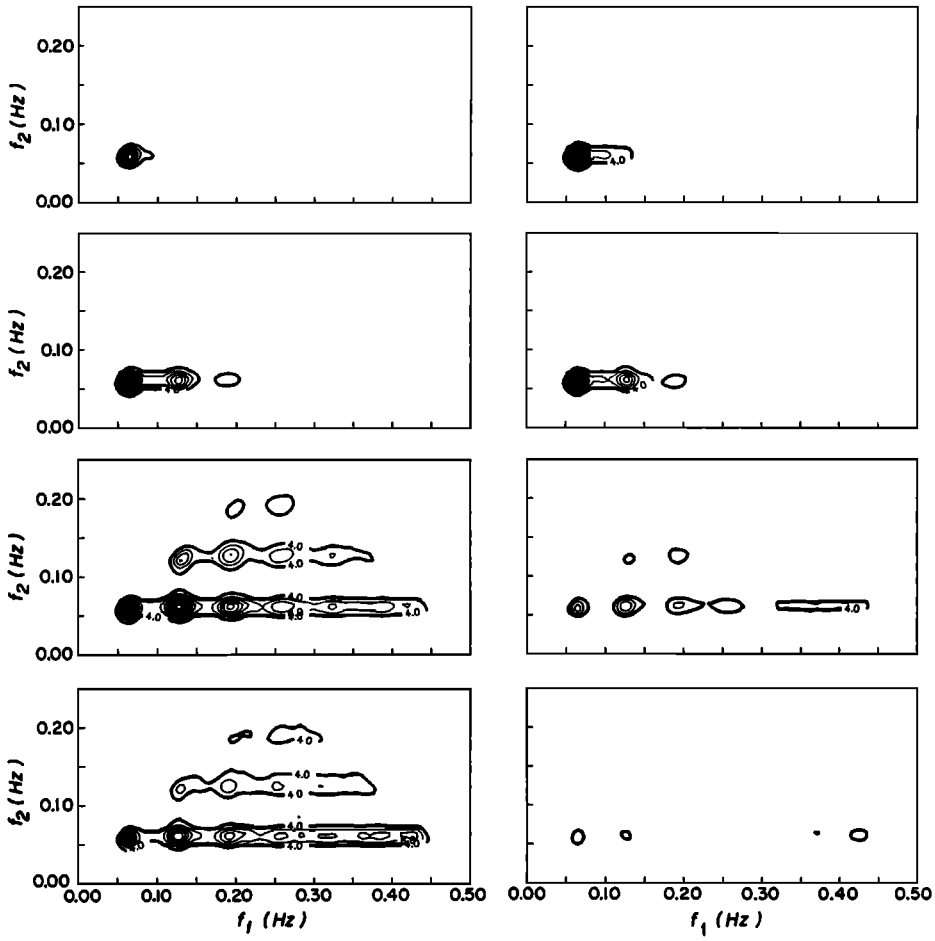

Fig. 7. (left) Real and (right) imaginary parts of the bispectrum of acceleration for February 2. The values are normalized such that the volume under the surface is proportional to the normalized skewness or asymmetry of acceleration. The minimum contour is 4.0, with contours every 4.0. Approximate depths are, from top to bottom, h = 6.3, 3.3, 1.5, and 0.9 m.

to about 4 and 10 times the frequency of the surface elevation spectral peak, respectively (Figure 5).

Surf beat contributes virtually nothing to acceleration variance and little to velocity variance in the outer surf zone, in contrast to its significance in swash elevation and velocity spectra [*Oltman-Shay and Guza*, 1987, and references therein]. Since surf beat motions are, by definition, low frequency, their time rates of change are small. Thus accelerations due to surf beat are insignificant when compared with accelerations due to higher-frequency motions.

4. Skewed and Asymmetric Accelerations

Although both u and u_t are approximately symmetric about horizontal and vertical axes at the 6-m station, both are obviously asymmetrical in shallower water (Figure 2). Linear theory predicts that initially symmetric waves remain symmetric as they shoal. Thus the observed asymmetries in u and u_t are manifestations of nonlinearities that grow as the waves shoal and break. The horizontal and vertical asymmetries are characterized here by skewness S and asymmetry A, third-order moments which are related to the wave shape [*Masuda and Kuo*, 1981; *Elgar and Guza*, 1985*b*]. With $H(u(t))$ the Hilbert transform of a velocity time series $u(t)$ and angle brackets denoting averaging,

$$S(u(t)) = \langle u^3(t)\rangle / \langle u^2(t)\rangle^{3/2} \tag{1a}$$

$$A(u(t)) = -S(H(u(t))) \tag{1b}$$

[cf. *Elgar*, 1987]. S and A measure asymmetry about horizontal and vertical axes, respectively. A "sawtooth" shape (steep front faces and gently sloping rear faces, but crests and troughs of equal amplitudes) has $S = 0$ and $A \neq 0$, while a "Stokes wave" shape (broad, low troughs and narrow, tall crests but symmetric front and back faces) has $S \neq 0$, $A = 0$.

As shown in Figure 6, the sawtoothlike shape of the cross-shore velocity of near-breaking and breaking waves (Figures 2*b*–2*d*) results in $A(u) > S(u)$ for depths of less than about 4 m. *Freilich and Guza* [1984] and *Elgar and Guza* [1985*b*, 1986] have shown that nonlinear triad interactions are responsible for the evolution of asymmetric sea surface elevations and velocities in shoaling waves (i.e., $A(u) > S(u)$ as the waves shoal). Since $S(u)$ (but not $A(u)$) terms appear in velocity-based sediment transport models [e.g., *Bowen*, 1980; *Bailard*, 1981], much of the nonlinearity in the velocity field may not contribute to net sediment transport. On the other hand, consistent with the more Stokeslike shape of the acceleration time series, $S(u_t) > |A(u_t)|$ (for the coordinate system used here, $A(u_t)$ is

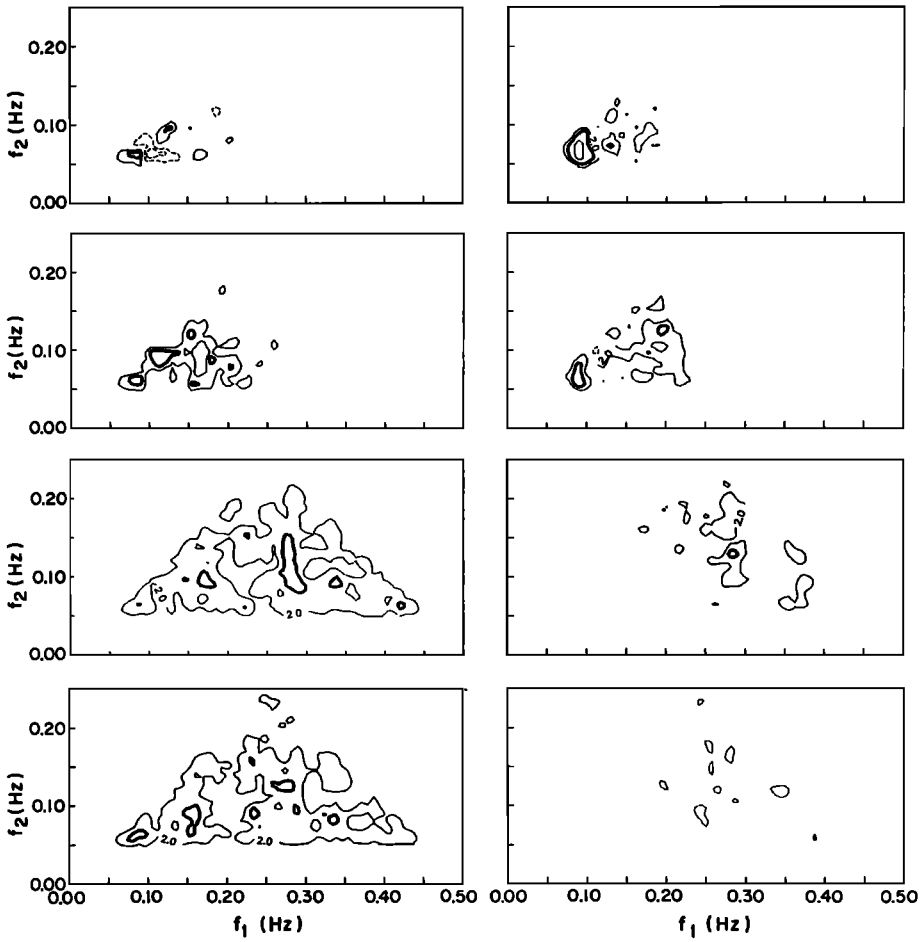

Fig. 8. Same as Figure 7, except for February 15. The minimum contour is 2.0, with contours every 2.0. The dashed contours in the top left panel indicate negative values (− 2.0). Approximate depths are, from top to bottom, h = 5.9, 2.9, 1.5, and 0.9 m.

negative) in shallow water. The acceleration field is very strongly skewed ($S(u_t) > 2$) toward large shoreward accelerations. Unnormalized third moments, also shown in Figure 6, reflect changes in wave height during shoaling and breaking as well as changes in wave shapes.

Just as the power spectrum describes the distribution of variance in frequency space, the bispectrum identifies the distribution of third moments in bifrequency space [*Hasselman et al.*, 1963]. Skewness and asymmetry are the integrals of the real and imaginary parts of the bispectrum, respectively. Examination of the bispectrum thus allows identification of wave triads (regions of bifrequency space) that are contributing strongly to the net integrated skewness and asymmetry.

Elgar [1987] shows

$$B_{1,2}(u_t) = -i\omega_1\omega_2\omega_3 B_{1,2}(u) \qquad (2)$$

where $B_{1,2}$ is the bispectrum for the triad consisting of the Fourier components with frequencies ω_1, ω_2, and $\omega_3 = \omega_1 + \omega_2$. Thus owing to the factor of i in (2), if the velocity field is strongly skewed, then the accelerations generally will be highly asymmetric (Figure 6), and vice versa.

Bispectra of acceleration are shown in Figures 7 (February 2) and 8 (February 15) for several depths. At 6-m depth (top panels), contributions to both skewness and asymmetry are restricted to near-degenerate triads composed of two waves with frequencies very near the peak of the velocity spectrum and a third wave at the first harmonic of the primary peak (see Figure 4) on both days. On February 2 (Figure 7), both the skewness and the asymmetry at all depths result principally from triads containing only waves at the peak frequency or its harmonics. On February 15, however, contributions to skewness come from triads containing a broad range of frequencies, while contributions to asymmetry come from triads containing ever higher-frequency waves as the depth decreases prior to wave breaking.

It is clear from both data sets that triads containing waves with frequencies below that of the peak in the velocity spectrum contribute very little to third moments of acceleration. Furthermore, both data sets illustrate the increasing importance of triads containing high-frequency waves as depth decreases. Thus third moments of acceleration (Figure 9) are more sensitive to the high-frequency cutoff than is the variance of acceleration (Figure 5), particularly for the relatively broad band February 15 data.

5. Discussion and Conclusions

The data discussed here are from a beach with moderate slope, and they span relatively small ranges of incident wave heights (60–95 cm), peak periods (13–17 s), and depths at the seaward edge of the breaking region (1.3–1.6 m). With signifi-

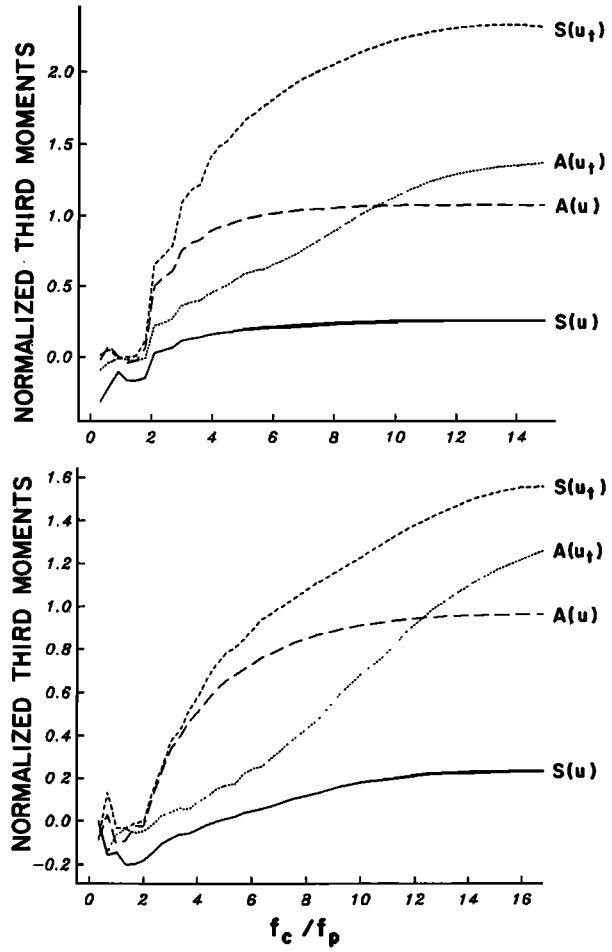

Fig. 9. Normalized third moments versus the ratio of high-frequency cutoff f_c to the power spectral peak frequency f_p for (top) February 2 ($f_p = 0.067$ Hz) and (bottom) February 15 ($f_p = 0.059$ Hz) in approximately 1.5-m depth.

cantly different bathymetry or wave conditions, velocity and acceleration statistics will evolve differently. The depth dependences shown here (e.g., Figures 3 and 6) are illustrative of a particular, but not uncommon, nearshore environment. The present results for acceleration spectra and bispectra contrast with similar analyses of velocity and sea surface elevation [*Elgar and Guza*, 1985*b*]. For example, triads involving a surf beat frequency can result in a velocity skewness roughly comparable to the skewness resulting from interactions between the power spectral peak frequency and its higher harmonics. However, surf beat contributes virtually nothing to field values of skewness and asymmetry of acceleration seaward of the swash zone. The significance of surf beat to sediment transport will be much diminished if accelerations, rather than velocities, are of first-order importance.

The very high frequency (e.g., > 0.4 hz) waves which contribute significantly to third moments of acceleration are of considerably less importance to third moments of velocity or sea surface elevation [*Elgar and Guza*, 1985*b*, Figure 10]. It is certainly obvious that high-frequency components contribute relatively more to acceleration variance than to velocity variance. It was not a priori certain, however, that high-frequency components are phase coupled to lower frequencies, thereby contributing significantly to the third-order acceleration statistics such as skewness and asymmetry. These third-order moments may be of importance to net sediment transport.

Accelerations associated with asymmetric (i.e., steep forward faces) waves differ significantly from accelerations due to Stokeslike waves having symmetry about the vertical axis. For asymmetric waves, peak accelerations occur during passage of the wave face, when horizontal velocities are both onshore and offshore. Decelerations are also seen to be weak relative to accelerations (Figures 2*c* and 2*d*). For Stokeslike waves, maximum accelerations and decelerations have approximately equal magnitudes, and both occur during passage of the wave crest, when velocities are onshore. The measurements of *Hanes and Huntley* [1986], obtained from a location well seaward of the break zone, show this Stokeslike behavior, as do data from the deepest station reported here (Figure 2*a*). Clearly, a time-dependent sediment transport model (including acceleration terms) is necessary to evaluate quantitatively to the significance of the relative phasing between acceleration and velocity fields.

The observed sensitivity of second and third moments of acceleration to the high-frequency cutoff (Figures 5 and 9) suggests that simplified evolution models with only a primary wave and a first harmonic [e.g., *Mei and Ünlüata*, 1972; *Elgar and Guza*, 1986] cannot accurately describe the evolution of the acceleration statistics occurring during wave shoaling. The need to include many harmonics may preclude the use of relatively simple model equations and their analytic solutions.

Acknowledgments. Support for this analysis was provided by National Science Foundation (NSF) grant OCE-8612008. The data collection was supported by the Office of Naval Research and the Sea Grant Nearshore Sediment Transport Study (project RICA-N-40). E. B. Thornton, R. L. Lowe, and R. J. Seymour contributed significantly to the field experiment. Portions of this research were performed at the Jet Propulsion Laboratory, California Institute of Technology, under contract to the National Aeronautics and Space Administration. Computations were performed at the San Diego Supercomputer Center, supported by NSF.

REFERENCES

Bailard, J. A., An energetics total load sediment transport model for a plane sloping beach, *J. Geophys. Res.*, *86*, 10,938–10,954, 1981.

Bowen, A. J., Simple models of nearshore sedimentation; Beach profiles and longshore bars, The Coastline of Canada, edited by S. B. McCann, *Geol. Surv. Pap. Geol. Surv. Can.*, *80-10*, 1–11, 1980.

Elgar, S., Relationships involving third moments and bispectra of a harmonic process, *IEEE Trans. Acoust. Speech, and Signal Processing*, *12*, 1725–1726, 1987.

Elgar, S., and R. T. Guza, Shoaling gravity waves: Comparisons between field observations, linear theory, and a nonlinear model, *J. Fluid Mech.*, *158*, 47–70, 1985*a*.

Elgar, S., and R. T. Guza, Observations of bispectra of shoaling surface gravity waves, *J. Fluid Mech.*, *161*, 425–448, 1985*b*.

Elgar, S., and R. T. Guza, Nonlinear model predictions of bispectra of shoaling surface gravity waves, *J. Fluid Mech. 167*, 1–18, 1986.

Ewing, J. A., M. S. Longuet-Higgins, and M. A. Srokosz, Measurements of the vertical acceleration in wind waves, *J. Phys. Oceanogr.*, *17*, 3–11, 1987.

Freilich, M. H., and R. T. Guza, Nonlinear effects on shoaling surface gravity waves, *Philos. Trans. R. Soc. London, Ser. A*, *311*, 1–41, 1984.

Guza, R. T., E. B. Thornton, and N. Christensen, Jr., Observations of steady longshore currents in the surf zone, *J. Phys. Oceanogr.*, *16*, 1959–1969, 1986.

Hallermeier, R., Oscillatory bedload transport: Data review and simple formulation, *Cont. Shelf Res.*, *1*, 159–190, 1982.

Hanes, D., and D. Huntley, Continuous measurements of suspended sand concentration in a wave dominated nearshore environment, *Cont. Shelf Res.*, *6*, 585–596, 1986.

Hasselman, K., W. Munk, and G. MacDonald, Bispectra of ocean waves, in *Time Series Analysis*, edited by M. Rosenblatt, pp. 125–139, John Wiley, New York, 1963.

Masuda, A., and Y. Kuo, A note on the imaginary part of bispectra, *Deep Sea Res., Part A, 28*, 213–222, 1981.

Mei, C. C., and U. Ünlüata, Harmonic generation in shallow water waves, in *Waves on Beaches and Resulting Sediment Transport*, edited by R. Meyer, pp. 181–202, Academic, San Diego, Calif., 1972.

Oltman-Shay, J., and R. T. Guza, Infragravity edge wave observations on two California beaches, *J. Phys. Oceanogr., 17*, 644–663, 1987.

Thornton, E. B., and R. T. Guza, Surf zone longshore currents and random waves: Models and field data, *J. Phys. Oceanogr., 16*, 1165–1178, 1986.

S. Elgar, Electrical and Computer Engineering, Washington State University, Pullman, WA 99164.

M. H. Freilich, Jet Propulsion Laboratory, California Institute of Technology, Pasadena, CA 91109.

R. T. Guza, Center for Coastal Studies, Scripps Institution of Oceanography A-009, La Jolla, CA 92093.

(Received January 7, 1988;
accepted February 22, 1988.)